ADVANCED MATERIALS

Supporting Information

for *Adv. Mater.*, DOI 10.1002/adma.202211176

Large Magnetoresistance of Isolated Domain Walls in $La_{2/3}Sr_{1/3}MnO_3$ Nanowires

Gloria Orfila, David Sanchez-Manzano, Ashima Arora, Fabian Cuellar, Sandra Ruiz-Gómez, Sara Rodriguez-Corvillo, Sandra López, Andrea Peralta, Santiago J. Carreira, Fernando Gallego, Javier Tornos, Victor Rouco, Juan J. Riquelme, Carmen Munuera, Federico J. Mompean, Mar Garcia-Hernandez, Zouhair Sefrioui, Javier E. Villegas, Lucas Perez, Alberto Rivera-Calzada, Carlos Leon, Sergio Valencia and Jacobo Santamaria*

Supporting Information

Large magnetoresistance of isolated domain walls in LSMO nanowires.

Gloria Orfila[#, 1], David Sanchez-Manzano[#,2], Ashima Arora [3], Fabian Cuellar[1], Sandra Ruiz-Gómez[4], Sara Rodriguez-Corvillo[1], Sandra López[1], Andrea Peralta[1], Santiago J. Carreira[2], Fernando Gallego[1], Javier Tornos[1], Victor Rouco [1], Juan. J. Riquelme[5,6], Carmen Munuera[5,6], Federico J. Mompean[5,6], Mar Garcia-Hernandez [5,6], Zouhair Sefrioui[1,6], Javier E. Villegas[2], Lucas. Perez [1,7], Alberto Rivera-Calzada[1,6], Carlos Leon[1,6], Sergio Valencia[3,], Jacobo Santamaria[1,6].*

[1] GFMC. Dept. Física de Materiales. Facultad de Física. Universidad Complutense. 28040 Madrid, Spain

[2]Unité Mixte de Physique, CNRS, Thales, Université Paris-Saclay, 91767 Palaiseau, France

[3]Helmholtz-Zentrum Berlin für Materialien und Energie, 12489 Berlin, Germany

[4]Max Planck Institute for Chemical Physics of Solids, 01187 Dresden, Germany

[5]Instituto de Ciencia de Materiales de Madrid ICMM-CSIC 28049 Cantoblanco. Spain

[6]Unidad Asociada UCM/CSIC, "Laboratorio de Heteroestructuras con aplicación en spintrónica" 28140 Madrid, Spain

[7] Instituto Madrileño de Estudios Avanzados - IMDEA Nanociencia, 28049, Madrid, Spain

[*] Corresponding author

[#] Equal contributors

Structure of LSMO films and transport characterization of nanowires

X-ray Diffraction (XRD) and X-ray reflectivity (XRR) measurements were performed (Figure S1a) to ensure the epitaxial and crystalline high quality of the LSMO thin layers. Resistance vs temperature measurements were performed to make sure that nanofabrication did not degrade the LSMO properties. As can be observed in Figure S1b, the resistivity remains practically unchanged after patterning the nanowires and the Curie temperature remains above room temperature.

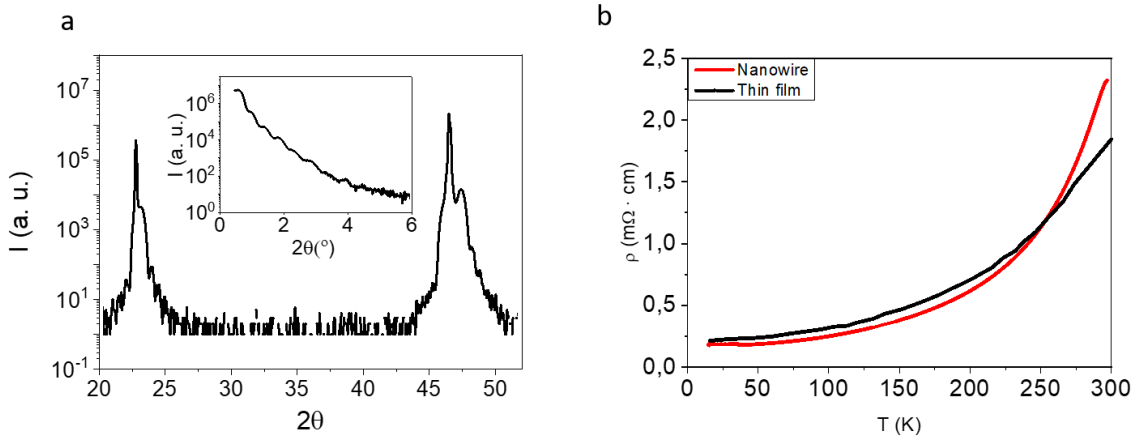

Figure S1. a) XRD and XRR of the LSMO sample before the etching process. b) Resistivity in function of temperature comparing the thin layer and the final nanostructured device. Resistivity is almost unchanged, showing the high quality of the nanowires.

XPEEM experiment on the 180 nm wire with the x ray beam directed along the contact leads (perpendicular to the nanowire)

By combining the information of the XMCD images taken at two orthogonal azimuth angles, a 2D map of magnetization angular distribution can be calculated, allowing for the identification of the magnetization directions of the device. To do so, XPEEM measurements with the X-ray beam directed along the wire direction were combined with XMCD images with the beam directed along the contact lead (perpendicular to the NW), see Figure S2. These measurements show that the contact wire cannot be switched by magnetic fields below 750Oe.

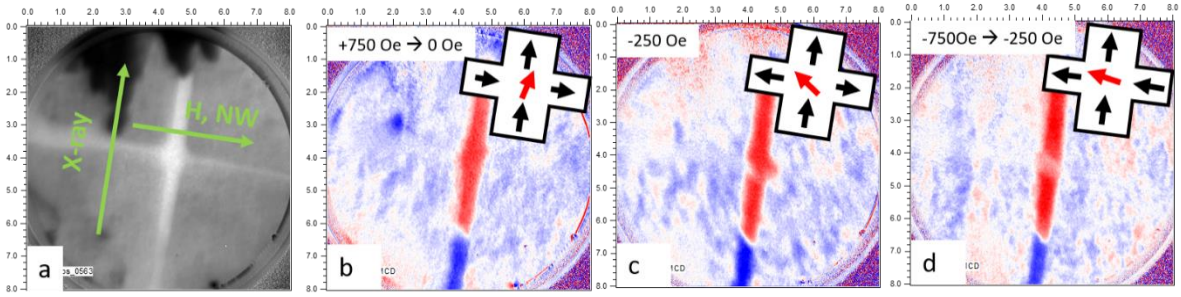

Figure S2. a) XAS of the device, with the magnetic field in the direction of the nanowire but with the X-ray beam in the direction of the contact wire. b-d) XMCD in the same configuration. With this configuration the magnetization of the contact can be probed. These measurements together with the ones in Figure 2 allows to unequivocally define the magnetization direction in our device.

A change in the magnetization of the cross can, nevertheless, be observed.

Rotation of the magnetization of the cross for the 180 nm wire

The relative angle at both sides of the domain wall between the cross and the wire reaches a maximum of 135°. XMCD images obtained at H = 237 Oe magnetic saturation at negative fields have been obtained at two azimuth angles of the sample (see panels a) and b) of Figure S3. In panel a) the beam is directed along the wire direction while in panel b) it is directed along the contact lead. A 2D map of the angular distribution of the magnetization can be obtained when considering that the XMCD is proportional to the projection of the

magnetization along the beam propagation direction. Panel c) depicts a 135° angular difference of the magnetization orientation at either sides of the domain wall.

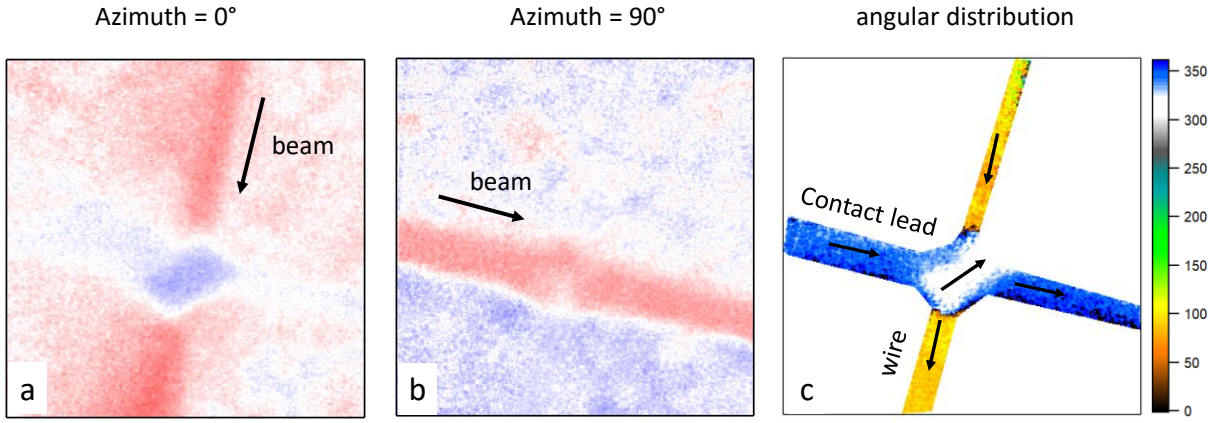

Figure S3 a) and b) correspond to XMCD images obtained centered at the cross at T = 50 K and H = +237.5 Oe after saturation at negative fields (H=-1000 Oe) for two orthogonal azimuth rotations of the 180 wide wire device. Black arrows indicate the direction of the incoming beam. Field of view 4 µm. c) Angular distribution of the magnetization as calculated from the XMCD images depicted in a) and b). Angular color scale on the right of panel c). Notice that the relative angle between the cross and the wire reaches 135 degrees.

XPEEM experiment on the 105 nm wire with the x-ray beam directed along the wire

XMCD images of magnetization switching were obtained for 105 nm wide wire (checked by means of AFM imaging). The experimental geometry is illustrated in panel a) together with an AFM image of the cross. The magnetic field and the x-ray beam were both aligned with the wire direction. Panel b) shows an XMCD image taken in remanence after saturating the sample in a +1000 Oe field. No change is observed in the wire/cross magnetic domain state after further decreasing the field to -350 Oe, maximum negative field value possible during imaging (Figure S4c). Panel d shows and XMCD image obtained at -350 Oe. After a magnetic field pulse of -500 Oe was applied. The pulse was enough to trigger a full reversal of the magnetization at the cross only. This is confirmed by the XMCD profile depicted in panel f across the cross which shows and XMCD equal in absolute value at the wire and the cross (ca.

0.035) but with opposite sign due to the different orientation of the magnetization projection along the beam direction. Higher magnetic field pulses lead to the propagation of the magnetic DW generated at the cross/wire intersection (panel e).

Magnetization switching happens now at higher field values (500 Oe) than in the 180 nm wire (150 Oe), and, importantly, the angle between magnetic moments is now larger (180º instead

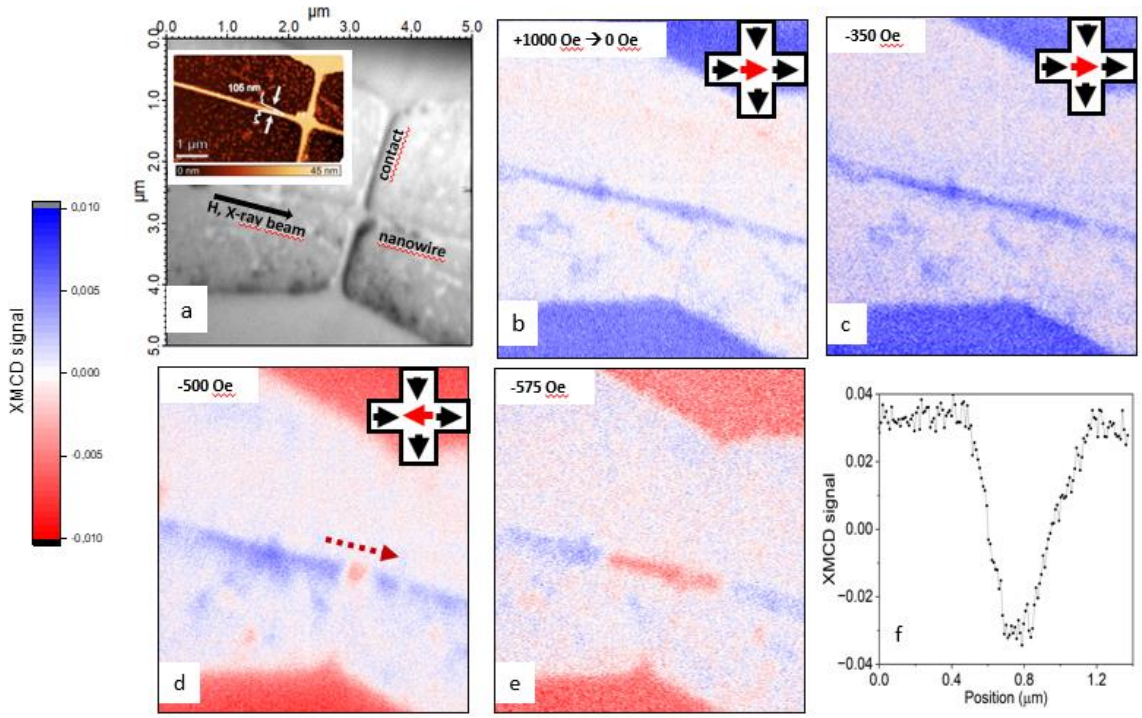

Figure S4 (a) XAS image of the cross with 100 nm nanowire. X-ray beam and magnetic field are oriented along the nanowire direction (perpendicular to the contact lead). Black contours in the image are due to shadows of the x ray beam. Inset depicts AFM from which the width of the wire has been determined b-e) XMCD images of the cross for different applied fields, blue (red) colours refer to magnetization (anti)parallel to the beam. Magnetic fields used to magnetize the wire are displayed in the legend, but for instrumental reasons measurements in panel c) to e) are conducted under -350 Oe after a magnetic field pulse as indicated in the insets is applied. Panel b shows an XMCD image taken in remanence after saturating the sample in a positive field. At -350 Oe, when magnetic field is inverted, the wire appears still uniformly magnetized (panel c). At -350 Oe, after a pulse of -500 Oe, the magnetization at the cross switches 180° (panel d) what triggers DW nucleation in the wire (panel e). (f) Dashed line shows the XMCD intensity profile along the wire and the cross following the direction indicated by the dotted line in panel d).

of 135 º).

Biaxial magnetocrystalline anisotropy of LSMO films.

We have examined the temperature dependence of the magnetocrystalline anisotropy. Transport in the wires is strongly influenced by the shape anisotropy and by domain wall magnetoresistance. To isolate the effect of the magnetocrystalline anisotropy MCA in the wires, we have measured magnetotransport in much wider (500 micron) Hall bars varying the angle between (in plane) magnetic field and wire (current) direction. When angle between current and magnetic field is varied anisotropic magnetoresistance tracks the effect of MCA. Results are shown in Supplementary Figure S5.

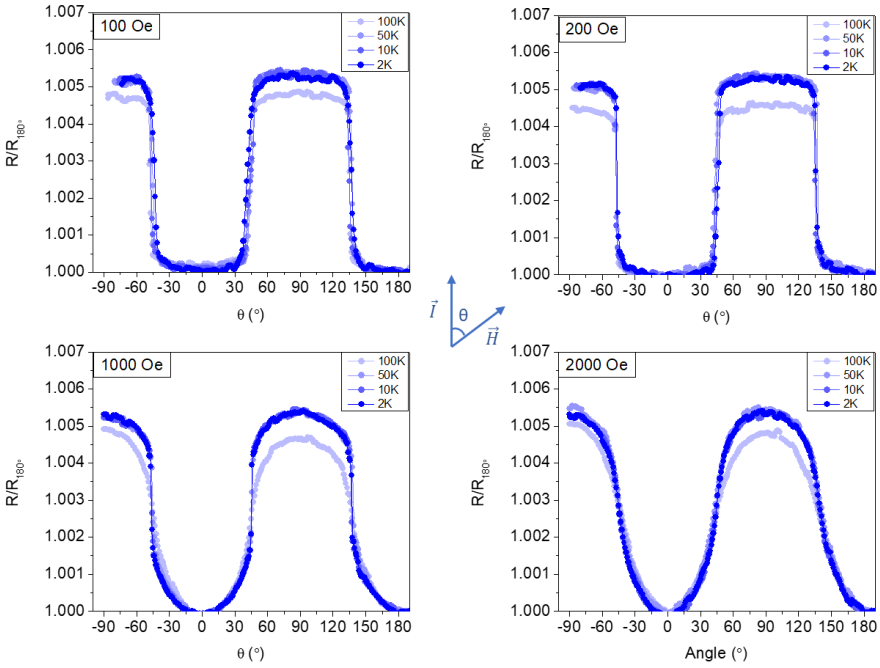

Figure S5. (Anisotropic) Magnetoresistance driven by the variation of the angle between in plane magnetic field and current direction in a 500 μm wide Hall bar (see sketch). Measurements are done at 2, 10, 50 and 100 K for magnetic fields of 100, 200, 1000 and 2000 Oersted. Figure shows the average of scans performed increasing and decreasing the angle between magnetic field and current direction.

Notice the dominant effect of the magnetocrystalline anisotropy with biaxial [110] easy axes for 100 and 200 Oe persisting in the whole temperature range. This explains the tendency of

magnetic moments at the cross to rotate towards [110] easy axes directions revealed by the SPEEM and MFM measurements of Figures 1 and 2 of the main text.

Contacts configuration for transport measurements.

Sketch illustrating the transport measurement configuration measuring voltage in the transverse leads with the in-plane magnetic field applied along the [100] wire long axis. In this configuration we probe the resistance of the wire segment between the transverse leads and the 2 DW (one at each cross) at their intersection NW

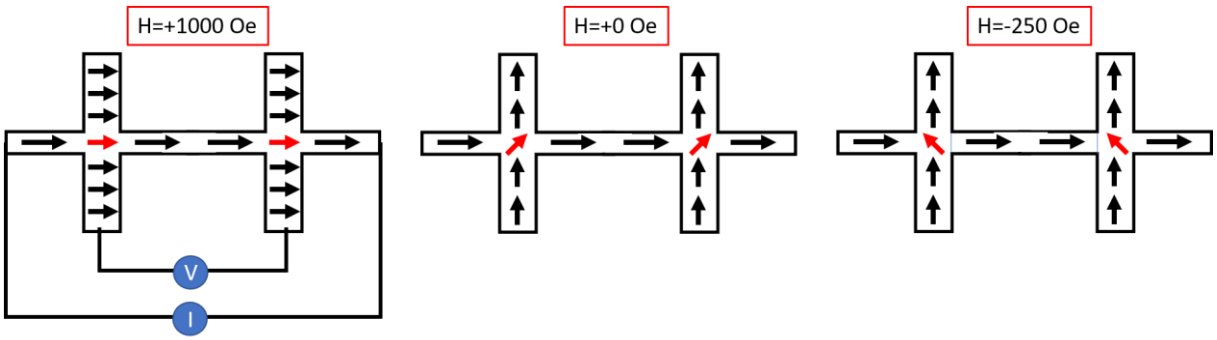

Figure S6. Measurement configuration of the cross-shape samples, indicating the direction of the magnetization in the nanowire, cross and contact wire.

Transport measurements on a 500 nm wide nanowire.

We have measured the MR of a wire 500nm wide and found very small values in the range of 0.1 % (see Figure S6). While in the case of the 65 and 180 nm wires we discuss the variation of MR in terms of increase of the angle between moments at both sides of the domain wall when the wire width is reduced, the case of the 500 nm is probably different as the shape of the MR curves suggest a different mechanism of magnetic switching.

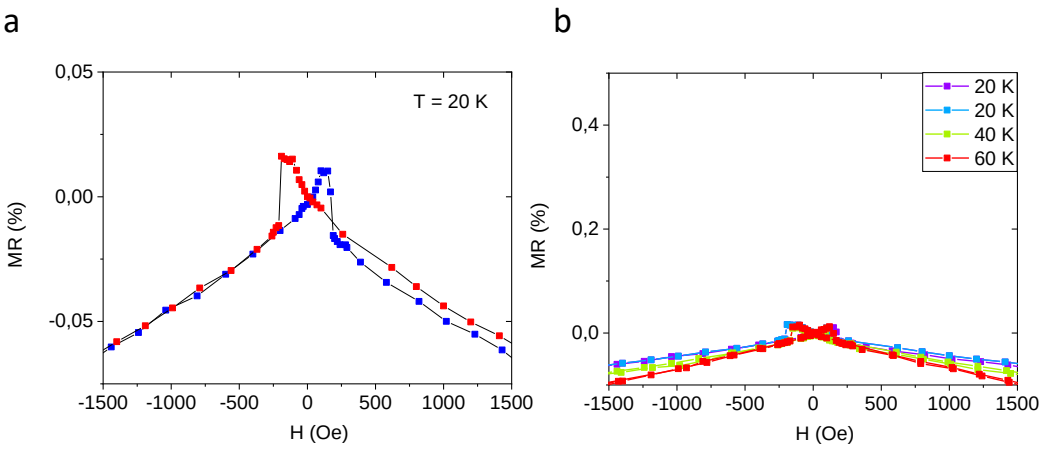

Figure S7 a) Magnetoresistance vs field MR(H) of a 500 nm wide nanowire at 1 μA with magnetic field directed along the wire direction at T=20K. b) Magnetoresistance at different temperatures between 20 and 60 K (see legend).

Heating effect: dependece of resistance on the injected current

Heating could be readily detected thanks to the pronounced temperature dependence of the LSMO resistivity. Heating has been detected at current values in excess of 10 μA though its effect increasing the background resistance. See **Figure S7**. Notice that increasing current produced a decrease of the switching field through the influence of heating effect. Also increased current yielded a reduction of the magnetoresistance effect more pronounced than the one expected from heating, indicating a current effect on the spin accumulation probably by spin torque. To avoid heating current level was kept between 0.1 and 1 μA which yields current densities in the range $10^3 - 10^4$ A/cm^2.

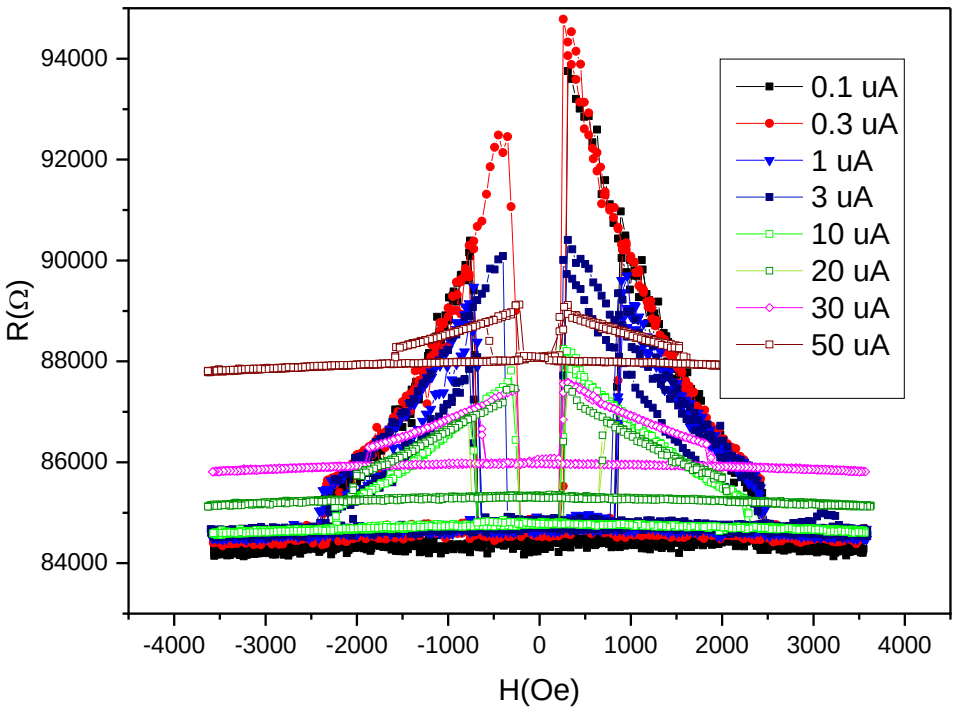

Figure S8. a) Resistance vs field of a 65 nm wire for different current levels between 0.1 and 50 μA (see legend). Notice that significant heating effect are observed only for currents in excess of 10 μA.